

METHODS FOR NITRIC OXIDE DETECTION DURING PLANT–PATHOGEN INTERACTIONS

E. Vandelle *and* M. Delledonne

Contents

1. Introduction	576
2. Nitric Oxide Detection by Mass Spectrometry	577
2.1. Procedure	577
2.2. Results	578
2.3. Comments	579
3. Nitric Oxide Detection by Laser Photoacoustic Spectroscopy	579
3.1. Procedure	579
3.2. Results	581
3.3. Comments	581
4. Nitric Oxide Detection by Chemiluminescence	582
4.1. Procedure	582
4.2. Results	583
4.3. Comments	583
5. Nitric Oxide Detection by Hemoglobin Conversion	583
5.1. Procedure	583
5.2. Results	584
5.3. Comments	584
6. Nitric Oxide Detection by Electron Paramagnetic Resonance (EPR) Spin Trap	585
6.1. Procedure	585
6.2. Results	586
6.3. Comments	587
7. Nitric Oxide Detection Using Diaminofluoresceins	587
7.1. Procedure	588
7.2. Results	589
7.3. Comments	589
8. Conclusion	590
References	591

Dipartimento Scientifico e Tecnologico, Università degli Studi di Verona, Verona, Italy

Methods in Enzymology, Volume 437
ISSN 0076-6879, DOI: 10.1016/S0076-6879(07)37029-8

© 2008 Elsevier Inc.
All rights reserved.

Abstract

Nitric oxide (NO) is involved in the transduction of numerous signals in living organisms, and its biological effects are often influenced by its concentration. Therefore, the ability to reliably detect and quantify NO is crucial to understanding its role in cellular processes. Many techniques are available to detect and quantify NO, but depending on the material and the aim of the analysis, specific adaptations are often required because its high chemical reactivity leads to the formation of numerous reactive nitrogen species that make the accurate determination of NO levels difficult. Moreover, the pathogen-induced hypersensitive response leads to high rates of reactive oxygen species production that react with NO and lead to the formation of its oxidized derivatives. The aim of this chapter is to provide an overview of the methods that have so far been employed to detect and measure NO in plants during the hypersensitive disease resistance response.

1. INTRODUCTION

Nitric oxide (NO) is a bioactive molecule that regulates an ever-growing list of biological processes in phylogenetically distant species (Beligni and Lamattina, 2001). In addition to acting as a potent endogenous vasodilator and having a role in inflammation, thrombosis, immunity, and neurotransmission in animals, NO is also involved in diverse physiological processes in plants under normal growth conditions (germination, leaf senescence, root growth) and under stress situations, such as pathogen attack (Wendehenne *et al.*, 2004). As a modulator of plant disease resistance, it plays a central role in hypersensitive response (HR) establishment, characterized by rapid and localized cell death (Delledonne *et al.*, 2001). The discovery of NO with these important physiological functions has led to the development of various analytical methods for its detection and quantification. However, the accurate measurement of NO production is somewhat tedious. Indeed, NO is a gaseous free radical that is extremely labile and its short half-life (6–10 s) reflects its highly reactive nature because of the presence of an unshared electron. Its broad chemistry involves an interplay among three species differing in their physical properties and chemical reactivity: the nitrosium cation (NO^+), the radical (NO), and the nitroxyl anion (NO^-) (Neill *et al.*, 2003). Moreover, NO interacts rapidly with O_2 to yield a variety of nitrogen oxides: NO_2 , N_2O_3 , NO_2^- , and NO_3^- , collectively termed reactive nitrogen species (RNS). In addition, the amount of NO available is highly dependent on the redox state of the cell, which makes the detection of NO, and in particular in plants challenged by pathogens, difficult. Indeed, an early event in the HR is the generation of superoxide (O_2^-) and accumulation of hydrogen peroxide

(H₂O₂), referred to as the oxidative burst, which is necessary to trigger host cell death in cooperation with NO (Delledonne *et al.*, 2001). During this process, the cell undergoes significant changes in its redox state that contribute to modification of the reactivity of NO.

The diverse assays available to measure NO are based on its particular physical and chemical properties and have been first optimized on animal systems before adapting them for plant study. Some assays detect NO gas emitted from cells, as NO has a high capacity of diffusion across membranes, whereas others measure NO derivatives, such as N₂O₃, taking into account its high oxidative metabolism. Most methods have been already used to detect NO during plant–pathogen interactions. They are described herein and compared in terms of their accuracy and reliability in measuring NO in this context.

2. NITRIC OXIDE DETECTION BY MASS SPECTROMETRY

This technique is based on the diffusion of dissolved gases through a capillary and their identification with a benchtop mass spectrometer according to their different mass/charge ratios (m/z). Changes in NO levels are evaluated by changes in the abundance of mass 30, corresponding to NO ($m/z = 30$). This method, referred to as membrane inlet mass spectrometry (MIMS), was developed in animals using mammalian cell cultures, but has been subsequently adapted to study NO production in plant cell suspensions and combined with restriction capillary inlet mass spectrometry (RIMS) to detect NO released from intact plant leaves or small plants (Conrath *et al.*, 2004). The instrument setup is presented in Fig. 29.1.

2.1. Procedure

In MIMS, 10 ml of cell suspension is transferred into an aquatic chamber (10 ml volume) and maintained under continuous agitation using a magnetic stirrer. The dissolved gases released by cells diffuse through a semipermeable Teflon membrane (50 μ m), which then evaporate into the ionization chamber of a benchtop mass spectrometer (Conrath *et al.*, 2004).

In RIMS, intact plant leaves or small plants are introduced in a leaf/plant cuvette placed in a translucent chamber, in which a metal bellows pump ensures rapid and efficient mixture of the 120-ml gas phase. The dissolved gases produced by the plant diffuse from the gas phase through a thin restriction capillary (inner diameter: 0.1 mm, length: 2 m) directly into a benchtop mass spectrometer (Conrath *et al.*, 2004)

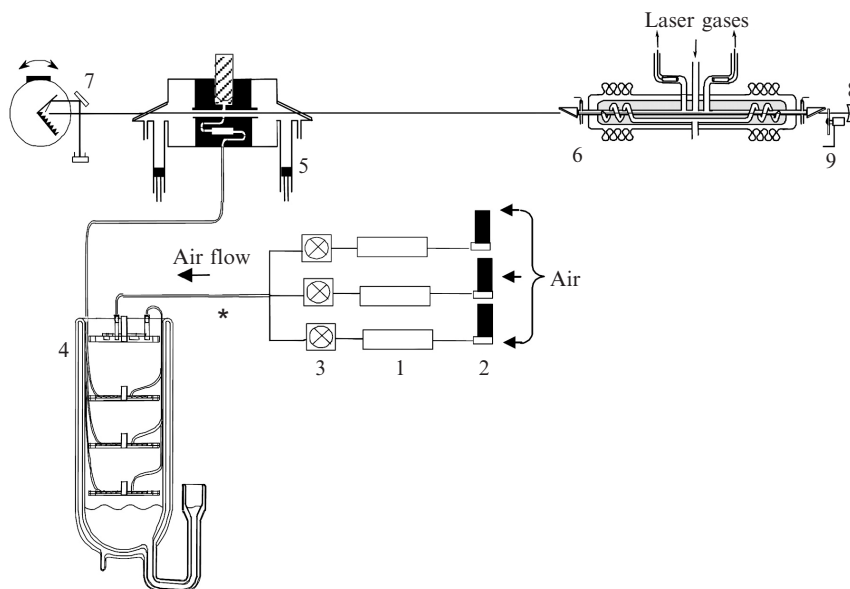


Figure 29.1 Experimental setup for COLPAD of NO. Up to three samples [typically, a bacterially challenged leaf, a mock (water)-injected leaf, and an instrumental control (baseline)] were sealed in three glass cuvettes (1), which could be sampled by alternating electronic valves (3). Airflow (1.5 liter h^{-1}) through the cuvettes was regulated by mass flow controllers (2). When not being sampled, the gas flow was vented from the cuvette to the atmosphere. Water vapor in the gas flow was removed using a Peltier cooling element (-5°) and a cold trap (-80° ; 4), prior to passage into the photoacoustic cell (5). The photoacoustic cell was inserted into a laser cavity to improve laser power and, thus, detection sensitivity. This laser cavity consisted of a gas discharge tube (6), a rotatable grating (7; for laser line selection), and a 100% reflecting mirror (8). To generate a photoacoustic signal, the laser light was modulated by a chopper (9; modulation frequency 1000 Hz). An additional water scrubber made of CaCl_2 (*) had no effect on the NO signal. Reproduced with permission from Mur *et al.* (2005).

2.2. Results

The specificity of the NO signal obtained by MIMS has been estimated using NO donors ($180 \mu\text{M}$), *S*-nitroso-*N*-acetyl-DL-penicillamine and *S*-nitroso-L-glutathione, and validated by the addition of the NO scavenger carboxy-2-phenyl-4,4,5,5-tetramethyl-imidazoline-1-oxyl-3-oxide ($150 \mu\text{M}$). The NO signal can be calibrated using NO-saturated water. The aqueous sample chamber is filled with 10 ml of water and is then flushed with N_2 for up to 5 min to purge the system of O_2 . At different time points, $5 \mu\text{l}$ of NO-saturated water (corresponding to a final NO concentration of $0.95 \mu\text{M}$) is added to the chamber. Under these conditions, Conrath *et al.* (2004) have estimated that 1 abundance unit at $m/z = 30$ corresponds to

10 to 13 pmol of NO. NO for signal quantification can also be generated by quantitatively reducing KNO_2 with KI (Berkels *et al.*, 2001).

Using MIMS, Conrath *et al.* (2004) have evaluated the amount of NO released by tobacco cells elicited by avirulent *Pseudomonas syringae* pv. *tomato*. They detected two NO bursts: the first at 1 h reaches 0.2 nmol of NO and the second more intense, occurring 4–8 h postinfection, presents a maximum around 0.5 nmol of NO (Conrath *et al.*, 2004).

2.3. Comments

The MIMS/RIMS method allows direct, fast, specific, and noninvasive online detection of NO and other gases in cell suspensions, as well as in entire leaves or plants. Moreover, this technique can be combined with an isotope tracing experiment, allowing source identification of gaseous NO by plant cells, as the isotopomers ^{14}NO and ^{15}NO can be distinguished. However, this method is less sensitive than other techniques such as photoacoustic laser spectroscopy (see later) and only allows the detection of extracellular NO.

A similar technique based on mass spectrometry has been used by Bethke *et al.* (2004) to analyze apoplastic NO production by plant tissues via the nonenzymatic reduction of nitrite. These authors describe a continuous sampling method where NO (and other gases) diffuses through a polyethylene membrane directly to the vacuum of the mass spectrometer.

3. NITRIC OXIDE DETECTION BY LASER PHOTOACOUSTIC SPECTROSCOPY

Laser photoacoustic detection (LPAD) is another direct-trace gas, noninvasive online sampling technique for measuring NO. This method is based on the photoacoustic effect, i.e., acoustic wave generation as a consequence of light absorption. Discontinuous laser illumination of a gas leads to temperature variations accompanied by pressure variations that create an audible sound detectable by a sensitive microphone (Mur *et al.*, 2005). The instrument setup is presented in Fig. 29.2.

3.1. Procedure

Samples are sealed in distinct glass cuvettes, which can be alternately sampled using electronic valves. Gases emitted from each sample are transported to the photoacoustic detection cell by an airflow ($1.5 \text{ liter}\cdot\text{h}^{-1}$) applied to sampling cells. To remove excess water vapor as a result of a temperature increase, gas samples pass into a Peltier cooling element (-5°) and a cold trap (-80°) prior to passage into the photoacoustic cell where

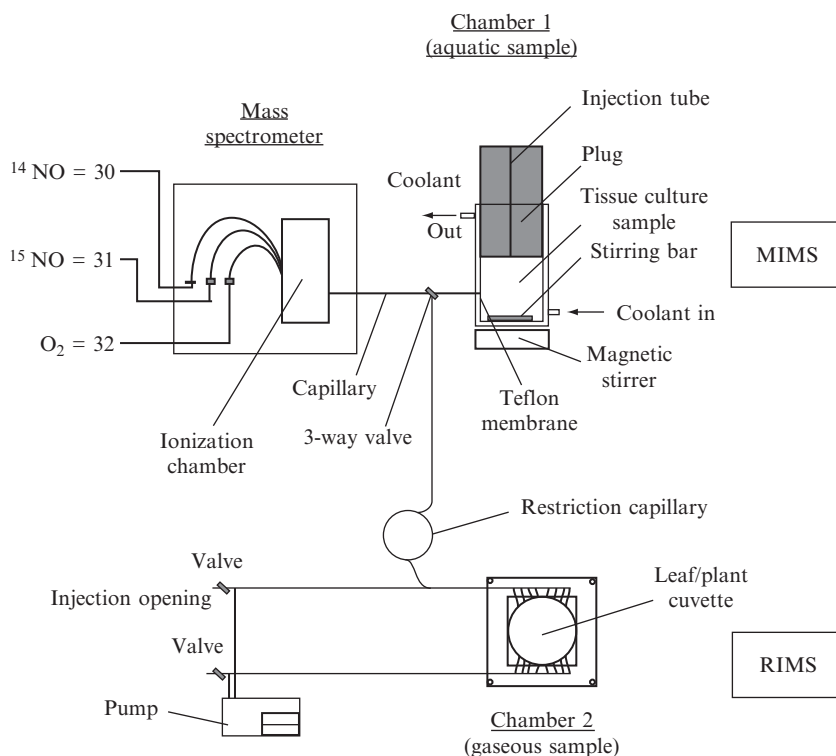


Figure 29.2 Schematic diagram of the experimental setup for MIMS/RIMS-based NO measurements. In MIMS, a cell suspension in an 8- to 10-ml reaction chamber was circulated over a thin ($50\ \mu\text{m}$) Teflon membrane by a magnetic stirrer. Dissolved gases, such as NO, diffused through the membrane and evaporated into the ionization chamber of a mass spectrometer. In RIMS, a metal bellows pump ensured rapid and efficient mixture of the 120-ml gas phase, which included the volume of a leaf cuvette ($8 \times 8 \times 0.4\ \text{cm}$). Before entering the mass spectrometer, NO and other gases passed a restriction capillary (inner diameter: $0.1\ \text{mm}$; length: $2\ \text{m}$). A three-way valve served to switch between the two sample chambers. Reproduced with permission from Conrath *et al.* (2004).

they are excited with a chopped carbon monoxide (CO) laser as a source of infrared light. To improve laser power, the photoacoustic cell is inserted into a laser cavity, consisting of a gas discharge tube, a rotatable grating (for laser line selection), and a 100% reflecting mirror. Five laser lines are used to measure NO concentration. Among them, the strongest one for NO measurement is at $1900.0426\ \text{cm}^{-1}$, and one is used to determine the water concentration in the sample (at $1790.6576\ \text{cm}^{-1}$).

Because there is a mixture of gases in the detection cell, and each gas has different absorption strength on every laser line, the mixed absorption

strength pattern is unraveled using a multicomponent matrix calculation algorithm. Results are presented as moles of $\text{NO}\cdot\text{h}^{-1}\cdot\text{g}^{-1}$ of fresh weight (if the amount of plant material has been determined at the beginning of the experiment) (Mur *et al.*, 2005).

3.2. Results

The sensitivity of the method has been assessed by applying known concentrations of NO to the airflow. In this way, a near 1:1 predicted/measured relationship between approximately 28 and 4.5 $\text{nmol}\cdot\text{h}^{-1}$ was observed (Mur *et al.*, 2005). The sensitivity and the reliability of the method *in planta* have been evaluated by infiltrating different concentrations of the NO donor sodium nitroprusside (SNP; 0.1 to 10 mM) in tobacco leaves. During the first hour postinfiltration, NO emission by plant was proportional to added SNP. Finally, the specificity of the NO signal has been confirmed by adding ozone to the air mixture, as NO readily forms NO_2 in the presence of O_3 : the addition of $0.2\text{ liter}\cdot\text{h}^{-1}$ NO to $1.3\text{ liter}\cdot\text{h}^{-1}$ airflow gives a photoacoustic signal that is completely abolished following the addition of $0.2\text{ liter}\cdot\text{h}^{-1}$ O_3 to the mixture (with a concomitant reduction in air to $1.1\text{ liter}\cdot\text{h}^{-1}$ to maintain a constant gas flow). In the same way, the NO signal due to SNP is abolished if O_3 is added to the gas flow after passing through the cuvette.

Using this method, Mur *et al.* (2005) have observed a rapid increase in NO production in tobacco leaves challenged with avirulent *P. syringae* pv. *phaseolicola*. This production, which occurs 40 min after infection, reaches about $17\text{ nmol NO}\cdot\text{h}^2\cdot\text{g}^{-1}$ fresh weight after 1 h.

3.3. Comments

A similar technique has been employed by Leshem and Pinchasov (2000) to determine relative endogenous NO content during the ripening of strawberries. In this work, the authors used a CO_2 laser to excite samples placed in a transparent sample cuvette at room temperature (22°C) in fluorescent light at $150\ \mu\text{M}\cdot\text{s}^{-1}\cdot\text{m}^{-2}$ intensity. To prevent NO_2 formation that may occur in air, the sample cuvette was filled with N_2 prior to NO measurement.

Laser photoacoustic detection displays a high sensitivity, with approximately $21.3\text{ pmol}\cdot\text{h}^{-1}$ that could be measured accurately and which is equivalent to thresholds for chemiluminescent detection (Archer, 1993); greater than 10-fold increased sensitivity compared to RIMS is seen (Conrath *et al.*, 2004). However, because LPAD detects NO in a gas mixture emitted from plants, it does not allow intracellular NO measurements.

4. NITRIC OXIDE DETECTION BY CHEMILUMINESCENCE

The concentration of NO can be determined using a simple chemiluminescent reaction involving ozone to produce oxygen and nitrogen dioxide:



This reaction produces light (chemiluminescence) that can be measured using a photodetector. The amount of light produced is proportional to the amount of NO in the sample. The assay takes advantage of the low solubility of NO in aqueous solution by measuring NO in the gas phase. This technique has been described in detail elsewhere (Planchet and Kaiser, 2006; Planchet *et al.*, 2005, 2006), as follows.

4.1. Procedure

For experiments with detached leaves, leaves are cut off from the plant and immediately placed in nutrient solution (adapted to studied plants), where the petiole is cut off a second time below the solution surface. The leaves (petiole in nutrient solution) are placed in a transparent lid chamber with 2 or 4 liters air volume, depending on the leaf size and number. A constant flow of measuring gas (purified air or nitrogen) of $1.5 \text{ liter} \cdot \text{min}^{-1}$ is pulled through the chamber and subsequently through the chemiluminescence detector [detection limit 20 parts per trillion (ppt); 20-s time resolution] by a vacuum pump connected to an ozone destroyer. The ozone generator of the chemiluminescence detector is supplied with dry oxygen (99%). The measuring gas (air or nitrogen) is made NO free by conducting it through a custom-made charcoal column (1 m long, 3 cm internal diameter, particle size 2 mm). Calibration is routinely carried out with NO free air (0 ppt NO) and with various concentrations of NO (1–35 ppb) adjusted by mixing the calibration NO gas (500 ppb in nitrogen) with NO-free air. Light is provided by a 400-W Hqi lamp above the cuvette. Quantum flux density is adjusted within limits ($150\text{--}400 \mu\text{mol} \cdot \text{m}^{-2} \cdot \text{s}^{-1}$ photon flux density) by changing the distance between lamp and cuvette. Air temperature in the cuvette is monitored continuously and is usually about 20° in the dark and $23\text{--}25^{\circ}$ C in the light.

For measurement of NO production from cell suspensions (10 ml), solutions are placed in small glass beakers of suitable size, located in a transparent lid chamber (1 liter gas volume) mounted on a shaker. NO is then measured by chemiluminescence detection as described earlier.

4.2. Results

Gaseous NO or aqueous solutions containing various amounts of NO can be used to calibrate the experiment. For example, based on the solubility of pure NO in water (1.9 mM at atmospheric pressure and 22° C), the equilibrium solution of a buffered solution (100 mM HEPES, pH 7.5) flushed for 15 min with 100 ppm NO gas contains 190 pmol NO·ml⁻¹ (Planchet and Kaiser, 2006; Planchet *et al.*, 2006). Aliquots of this solution are rapidly injected under a gas stream of air or nitrogen into a small beaker with buffer solution mounted in the headspace cuvette on a magnetic stirrer, and the NO released is detected by chemiluminescence. It has been reported that the integrated amount of NO detected by this method is practically identical to the theoretical NO content (Planchet and Kaiser, 2006).

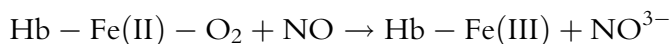
This technique does not detect NO production in cryptogein-treated leaves, although it has been shown to reveal NO emission from tobacco cells treated with the elicitor cryptogein (Planchet *et al.*, 2006). In the latter case, however, NO production was detected only after a 3- to 6-h treatment and was not affected by NOS inhibitors, contrary to previous results obtained with 4,5-diaminofluorescein diacetate (DAF-2 DA) staining (Lamotte *et al.*, 2004; see Section 7).

4.3. Comments

The chemical properties of NO enhance the specificity of the assay. This method offers high sensitivity, around 20 pmol NO (Archer, 1993), and is quantitative at NO concentrations in the picomolar range. However, it does not allow for intracellular detection of NO, and results obtained with this method compared to other techniques are debatable.

5. NITRIC OXIDE DETECTION BY HEMOGLOBIN CONVERSION

This method is based on hemoglobin absorbance changes as a result of its conversion from oxyhemoglobin (HbO₂) to methemoglobin (metHb) in the presence of NO:



5.1. Procedure

For experiments with detached leaves (Orozco-Cardenas and Ryan, 2002), 200 mg of frozen leaves (harvested after treatment) is ground and homogenized in 1 ml of cooled buffer [0.1 M sodium acetate, 1 M NaCl, and

1% (w/v) ascorbic acid, pH 6.0]. The homogenates are centrifuged at 10,000 *g* for 20 min at 4° C, and the supernatants are clarified by passing through a 0.8 × 4-cm column in 1-X8 resin.

For experiments with cell suspensions (Clarke *et al.*, 2000; Delledonne *et al.*, 1998), cells are washed twice and resuspended at 0.1 g·ml⁻¹ in a minimum buffer (e.g., 50 mM MES, 75 mM sucrose, 1 mM CaCl₂, 1 mM K₂SO₄, pH 5.5; Clarke *et al.*, 2000). Following treatments, 1-ml aliquots of cells are removed at various time points. In each case, 1 ml of sample (clear leaf homogenate or cell suspension) is incubated for 5 min with 100 U catalase and 100 U superoxide to remove reactive oxygen intermediates that could interfere with the assay (Delledonne *et al.*, 1998).

It is important to note that the buffer should not contain any compounds that could absorb in the range of 390–430 or 560–610 nm. The HbO₂ solution stock is then added to samples to a final concentration between 5 and 10 μM. After 2–5 min of incubation (depending on the rate of NO production in the system under study), the rate of HbO₂ to metHb conversion is evaluated spectrophotometrically. If NO production is analyzed in cell suspensions, cells are pelleted by centrifugation at 10,000 *g* for 30 s prior to measuring the absorbance.

5.2. Results

The absorbance peak for HbO₂ at 415 nm shifts toward 406 nm for metHb. If a dual-wavelength spectrophotometer is available, measurements of the conversion are obtained by the difference absorbance of 401–411 nm ($\Delta\epsilon = 38 \text{ mM}^{-1}\cdot\text{cm}^{-1}$), 421–411 nm ($\Delta\epsilon = 39 \text{ mM}^{-1}\cdot\text{cm}^{-1}$), or 401–421 nm ($\Delta\epsilon = 77 \text{ mM}^{-1}\cdot\text{cm}^{-1}$). Using the last pair of wavelengths, the theoretical detection limit for NO is 1.3 nM. If only single wavelength readings are possible, 401 or 421 nm will give reliable data (Murphy and Noack, 1994).

Nitric oxide emission by plant cells infected with pathogens, i.e., a rapid and relatively weak NO burst (around 0.5 μM) after 30 min followed by a second one severalfold greater (2 μM), specifically induced in cells inoculated with the avirulent bacterial strain (Delledonne *et al.*, 1998), was first demonstrated using this method.

5.3. Comments

This assay has few technical requirements and has a NO detection threshold around 1 nM. However, it is prone to interference by ROS. The addition of superoxide dismutase and catalase as sample pretreatments can minimize this problem, but does not completely ensure the specificity of the method.

6. NITRIC OXIDE DETECTION BY ELECTRON PARAMAGNETIC RESONANCE (EPR) SPIN TRAP

Electron paramagnetic resonance detection is based on the fact that at a discrete amount of energy (microwave frequency) and magnetic field strength, unpaired electrons are promoted to higher energy levels; following this, the relaxation from this state produces a characteristic spectrum. Although NO is a paramagnetic molecule with an unpaired electron, it cannot be studied by simple EPR, as the relaxation time of the stimulated electron to the ground state is too rapid to be detected (Maples *et al.*, 1991). Therefore, EPR detection has been combined with spin trapping to stabilize the labile free radical and allow NO measurement. Different types of spin traps have been used to detect NO by EPR, but only those that have been used to measure NO emission during plant–pathogen interactions are described here. The spin-trapping agents used are diethyldithiocarbamate (DETC) and *N*-methyl-*D*-glucamine dithiocarbamate (MGD). Binding NO with hydrophobic Fe²⁺–dithiocarbamate complexes results in the formation of paramagnetic mononitrosyl iron complexes with dithiocarbamate that can be detected by EPR spectroscopy at 77 K and ambient temperature.

6.1. Procedure

6.1.1. Use of DETC

To overcome the problem of water solubility of the Fe²⁺(DETC)₂ complex, albumin should be added to the reaction mixture (Tsuchiya *et al.*, 1996). Moreover, the trapping reaction should be carried out in presence of Na₂S₂O₄ in order to avoid oxidation of iron and NO in the Fe²⁺(DETC)₂NO complex (Tsuchiya *et al.*, 1996).

For experiments performed with detached leaves (Huang *et al.*, 2004), about 0.6-g leaves frozen in liquid nitrogen are crushed with a mortar and pestle and incubated in 1.2 ml of buffered solution [50 mM HEPES, 1 mM dithiothreitol (DTT), 1 mM MgCl₂, pH 7.6] for 2 min. For experiments performed with cell suspensions (Zeidler *et al.*, 2004), 500 μl of cells are harvested at different time points after treatment and incubated in 0.6 ml of 50 mM HEPES, pH 7.6, 1 mM DTT, 1 mM MgCl₂, at 37° C for 2 min. In each case, the mixture is centrifuged at 13,000 *g* for 2 min. The supernatant is then added to 300 μl of freshly made Fe²⁺(DETC)₂ solution (2 M Na₂S₂O₄, 3.3 mM DETC, 3.3 mM FeSO₄, 33 mg·ml⁻¹ bovine serum albumin), incubated for 2 min at room temperature, and frozen in liquid nitrogen.

Electron paramagnetic resonance measurements are performed on a Bruker ESP300 X-band spectrometer under the following conditions:

room temperature; microwave power, 20 mW; modulation amplitude, 3 G; scan rate, approximately $2.5 \text{ G}\cdot\text{s}^{-1}$; time constant, 164 ms (Huang *et al.*, 2004; Zeidler *et al.*, 2004).

6.1.2. Use of MGD

N-Methyl-*D*-glucamine dithiocarbamate is a derivative of DETC (Komarov and Lai, 1995). It is readily soluble in water and forms a water-soluble $\text{Fe}^{2+}(\text{MGD})_2\text{NO}$ complex.

Extracts of leaves are obtained by homogenizing 170 mg of leaf tissue in 200 μl of phosphate buffer (100 mM, pH 7.2) using a Polytron mixture system (Kinematica AG; Modolo *et al.*, 2005). After centrifugation at 10,000 *g* for 10 min, the supernatant is incubated for 1 h at room temperature in an equal volume of 100 mM phosphate buffer containing $\text{Fe}^{2+}(\text{MGD})_2$ at 1 mM Fe^{2+} [stock solutions of $\text{Fe}^{2+}(\text{MGD})_2$ are prepared by dissolving MGD sodium salt and FeSO_4 in deionized water, with a molar ratio of 5:1, respectively]. Care should be taken to use this trap in anaerobic conditions to avoid oxidation of Fe^{2+} to Fe^{3+} , which results in loss of trap as well as subsequent production of superoxide that would interfere with NO measurement. Samples are then frozen, stored in liquid nitrogen, and thawed immediately before EPR analysis.

Electron paramagnetic resonance measurements are carried out with a Bruker EMX instrument under the following conditions: room temperature; microwave power, 20 mW; modulation amplitude, 2.5 G; scan rate, $2.4 \text{ G}\cdot\text{s}^{-1}$; time constant, 81.92 ms; gain, 2.0×10^5 (Modolo *et al.*, 2005).

6.2. Results

The $\text{NO-Fe}^{2+}(\text{DETC})_2$ complex gives a three-line EPR spectrum at room temperature ($g_{\text{iso}} = 2.04$; $a^{\text{N}} = 2.7 \text{ G}$; see Fig. 29.2). A calibration curve can be obtained using NaNO_2 as an NO source (reaction mixture: 3.3 mM Fe^{2+} , 3.3 mM DETC, 33 $\text{mg}\cdot\text{ml}^{-1}$ albumin, about 2 M $\text{Na}_2\text{S}_2\text{O}_4$, 0–10 μM NaNO_2). The intensity of the signal increases linearly with the NO concentration, with a correlation coefficient of 0.998 (Tsuchiya *et al.*, 1996). The NO donor SNP can also be used as a standard in the presence of excess $\text{Fe}^{2+}(\text{DETC})_2$ complex (Huang *et al.*, 2004; Tsuchiya *et al.*, 1996; Zeidler *et al.*, 2004). The concentration can be determined using peak intensity or by double integration.

Using EPR analysis with DETC as a spin-trapping agent, NO has been detected early in *Arabidopsis thaliana* cells elicited with lipopolysaccharides after 10 min (Zeidler *et al.*, 2004). These authors have observed the characteristic three-line spectrum, without quantifying the amount of NO produced.

The $\text{Fe}^{2+}(\text{MGD})_2\text{NO}$ complex has an EPR spectrum very similar to that of $\text{Fe}^{2+}(\text{DETC})_2\text{NO}$, i.e., a three-line spectrum with $g_{\text{iso}} = 2.04$, $a^{\text{N}} = 12.9 \text{ G}$ in aqueous solution. Quantification of the spin adduct can be performed using an aqueous solution of TEMPOL (4-hydroxy-2,2,6,6-tetramethyl piperidine *N*-oxyl) as a standard (Jasid *et al.*, 2006). TEMPOL solutions are standardized spectrophotometrically at 429 nm using $\epsilon = 13.4 \text{ M}^{-1} \cdot \text{cm}^{-1}$. Next, the concentration of the $\text{Fe}^{2+}(\text{MGD})_2\text{NO}$ adduct is obtained by double integration of the three lines and cross-checked with TEMPOL spectra.

Using this method with MGD as a spin-trapping agent, Modolo *et al.* (2005) have demonstrated NO emission in *A. thaliana* leaves in response to avirulent *P. syringae* pv. *maculicola* 6 h after infection and have shown the involvement of nitrite as a major source of NO during this process. In this study, however, the amount of NO produced was not determined.

6.3. Comments

Care must be taken in terms of the chemicals used to analyze NO production using EPR spectrometry. For example, L- N^G -nitroarginine methylester (L-NAME) is not a suitable inhibitor of NO synthase in measurement of NO by the $\text{Fe}^{2+}(\text{DETC})_2$ complex method, as under strong reductive conditions it shows the same spectrum of the $\text{Fe}^{2+}(\text{DETC})_2\text{NO}$ complex (Tsuchiya *et al.*, 1996). Also, the potential interference from nitrite must be considered. For instance, the use of reducing agents that convert NO_2^- back to NO results in overestimating the amount of free NO in aqueous solutions (Venkataraman *et al.*, 2002). Thus, the use of DETC as a spin trap that requires the addition of $\text{Na}_2\text{S}_2\text{O}_3$ in excess is not recommended and MGD is preferred. Finally, EPR does not allow easy continuous NO detection *in planta*.

7. NITRIC OXIDE DETECTION USING DIAMINOFLORESCEINS

This method is based on the reaction of aromatic amines with NO in the presence of dioxygen to produce the corresponding triazenes; the corresponding triazole ring compounds are generated spontaneously from aromatic vicinal diamines under neutral conditions (Nagano *et al.*, 1995). The most common probe is 4,5-diaminefluorescein, a fluorescein derivate (Kojima *et al.*, 1998). DAF-2 does not react directly with NO, but with the

N_2O_3 formed during the course of NO oxidation, according to the following reactions (Ignarro *et al.*, 1993):



The reaction between DAF-2 and the oxidation product of NO leads to formation of the highly fluorescent triazolofluorescein DAF-2T (Kojima *et al.*, 1998). For intracellular NO detection, the cell-permeable derivate of DAF-2, namely DAF-2 diacetate (DAF-2 DA), can permeate readily into cells where it is hydrolyzed by intracellular esterases to generate DAF-2 (Kojima *et al.*, 1998).

The fluorescence intensities of the triazole derivatives of DAFs are dependent on pH (Kojima *et al.*, 1999). 3-Amino-4-(*N*-methylamino)-2',7'-difluorofluorescein (DAF-FM) is an improved DAF analogue, which, after reaction with NO, results in the triazole DAF-FM T that shows stable and intense fluorescence in a wide range of pH values (Kojima *et al.*, 1999).

7.1. Procedure

Leaves are infiltrated with a 10 μM DAF-2 DA-containing solution (10 mM MES-Tris, 10 mM KCl, 0.1 mM CaCl_2 , pH 7.6), and 1 h after infiltration, the treated leaf areas are analyzed by confocal microscopy (Qu *et al.*, 2006). Alternatively, leaf segments (2 \times 2 mm) are mounted in MES buffer (10 μM MES, 50 μM KCl, pH 6.15) on a glass slide with a coverslip. Samples are immersed in 10 μM DAF-2 DA in MES buffer for 10 min in the dark at room temperature, rinsed in pure MES buffer to remove excess dye for another 10 min, and analyzed by microscopy (Prats *et al.*, 2005). Experiments can also be carried out with leaf epidermal sections produced from the abaxial or the adaxial surface (Foissner *et al.*, 2000; Gould *et al.*, 2003; Zeidler *et al.*, 2004). Leaf peels are incubated in a 10 μM DAF-2 DA- or 5 μM DAF-FM DA-containing solution (10 mM Tris, pH 7.0–7.2) for 10 to 30 min in the dark at room temperature. Sections are then removed and transferred to a dish of fresh loading buffer (without probe) to wash excess fluorophore for 10–20 min. Next, the samples are mounted on microscope slides, where they are still immersed in fresh loading buffer, and examined immediately by microscopy. Microscopic analyses on whole leaves or epidermal peels are usually carried out with a confocal laser microscope (488 nm excitation, emission spectrum comprised between 500 and 550 nm), but have also been performed using an epifluorescence microscope equipped with an FITC filter set (excitation, 490 nm; beam splitter, 510 nm; emission, 525 nm).

To detect NO in plant cell suspensions (Lamotte *et al.*, 2004; Planchet *et al.*, 2005, 2006; Vandelle *et al.*, 2006; Wang and Wu, 2004; 2005;

Yamamoto *et al.*, 2004), cells are washed in fresh culture medium or usual assay buffer and incubated in the same buffer containing 10 to 20 μM of DAF-2 DA for 15–60 min in the dark at room temperature under constant agitation. Next, cells are washed (once or twice) with fresh suspension buffer to wash off excess fluorophore. Cell treatments can be performed directly in the flask containing DAF-2 DA-loaded cells. In this case, aliquots (1 or 2 ml) of cells are taken at different times after treatment and analyzed for DAF-2T fluorescence (Planchet *et al.*, 2005, 2006; Wang and Wu, 2004, 2005; Yamamoto *et al.*, 2004). Alternatively, cell suspensions are transferred into a 24-well plate (1 ml per well) and treated in the dark. NO production is then measured using a plate reader fluorometer (Lamotte *et al.*, 2004; Vandelle *et al.*, 2006). NO production in cell suspensions is measured using a luminescence spectrophotometer or a spectrofluorometer (485 or 495 nm excitation, 510 or 515 nm emission).

7.2. Results

The formation of DAF-2T produces a green fluorescence attributable to the presence of NO in cells. DAF-2T fluorescence is expressed in relative units. As a positive control to test the efficiency of the staining, some samples are incubated in a solution containing an NO donor, in addition to the buffered DAF-2 DA. In contrast, as negative controls, in all types of experiments, samples are incubated in assay buffer lacking DAF-2 DA.

Using DAF-2 DA, Foissner *et al.* (2000) have reported on the real-time imaging of NO production in cryptogein-treated epidermal tobacco cells and have shown that NO accumulation and/or production by confocal microscopy analysis occurs early in chloroplasts, in the nucleus and along the plasma membrane, and in distinct cellular compartments in the vicinity of chloroplasts, most likely peroxisomes. A monophasic NO burst that occurs within a few minutes after elicitor treatment has been detected in tobacco cell suspensions elicited with cryptogein by measuring the fluorescence increase of DAF-2T using a plate reader fluorometer (Lamotte *et al.*, 2004).

3-Amino-4-(*N*-methylamino)-2',7'-difluorescein staining, combined with confocal laser-scanning microscopy, has been used to analyze the time course of NO production in *A. thaliana* cell suspensions elicited with lipopolysaccharides (Zeidler *et al.*, 2004). In this study, an increase in DAF-FM T fluorescence was observed as early as 2 min after elicitation.

7.3. Comments

4,5-Diaminefluorescein cross-reacts with dehydroascorbic acid (DHA) to produce fluorescent compounds, termed DAF-2-DHAs, while ascorbic acid considerably attenuates the formation of DAF-2T, probably by affecting the formation of N_2O_3 (Zhang *et al.*, 2002). In addition,

catecholamines, superoxide radical, dithiothreitol, 2-mercaptoethanol, glutathione, and divalent cations such as Ca^{2+} or Mg^{2+} can interfere with DAF-2 during NO detection (Broillet *et al.*, 2001; Nagata *et al.*, 1999). In order to avoid false-positive results, it is also necessary to check for any eventual autofluorescence detectable around 515 nm for all substances employed in the assay.

Decreased fluorescence of samples not protected from light even for a few minutes has been reported (Räthel *et al.*, 2003) and it is, therefore, strictly necessary to work in the dark when handling DAF-2 or DAF-2T samples.

4,5-Diaminefluorescein does not react in neutral solutions with other oxidized forms of NO, such as NO_2^- and NO_3^- , or with other ROS, such as O_2^- , H_2O_2 , and ONOO^- , providing specificity for NO detection (Kojima *et al.*, 1998). However, because DAF-2 does not react with the NO-free radical but rather with N_2O_3 , the fluorescence intensity depends on the rate of NO oxidation, which requires oxygen, making the use of DAFs under anoxia difficult.

By calibrating NO standard curves, it has been shown that the detection limit of NO by DAF-2 is 3–5 nM (Itoh *et al.*, 2000; Kojima *et al.*, 1998).

8. CONCLUSION

Ideally, methods for determination of NO should exhibit a high degree of sensitivity and specificity and should allow assessment of intra- and extracellular levels of NO from gas or liquid phases (Mur *et al.*, 2005). Even so, no assay described herein possesses all these ideal characteristics. Some techniques allow direct measurement of NO concentration, such as EPR spin trap, or indirect NO detection, for example, using DAF-2DA/DAF-FM staining. Other methods are suitable for NO detection in the gas phase, such as laser photoacoustic spectroscopy, chemiluminescence, or mass spectrometry. Another method consists of electrochemical detection of NO using a Clark-type NO electrode (Yamasaki *et al.*, 1999). This method has not been described in this chapter because it has never been used to study plant defense responses. All the other methods cited have, however, been used to study NO during plant–pathogen interactions, often leading to large discrepancies in the results, even for the same plant–pathogen system. For example, laser photoacoustic spectroscopy (Mur *et al.*, 2005), as well as DAF-2DA/FM staining (Foissner *et al.*, 2000; Lamotte *et al.*, 2004; Zeidler *et al.*, 2004) and chemiluminescence (Planchet *et al.*, 2006), revealed monophasic NO production in tobacco leaves or cells after elicitation. In contrast, when analyzed by MIMS, the same tobacco cells showed two NO bursts after avirulent *P. syringae* infection (Conrath *et al.*, 2004), as also observed in

elicited soybean cells by MIMS and by the oxyhemoglobin assay (Conrath *et al.*, 2004; Delledonne *et al.*, 1998). Moreover, even if both DAF-2DA staining (Lamotte *et al.*, 2004) and chemiluminescence (Planchet *et al.*, 2006) detected a monophasic pattern of NO production in cryptogein-treated tobacco cells, the former method detects these changes very early, after a few minutes of treatment, whereas the latter detects differences after a 6-h treatment. These discrepancies may be because of differences in sensitivity, specificity, and localization of NO detection. Taking into account the most important features that accurate methods for NO detection should possess, DAF-2DA/FM staining, which consists of measuring NO indirectly by detecting N₂O₃ (Kojima *et al.*, 1998), appears to be an easy and suitable technique. It is conceptually similar to the indirect measurement of NO by measuring nitrite levels using the Griess reaction or the aromatic diamino compound 2,3-diaminonaphthalene, which are commonly used to measure NO in animal systems (Nagano, 1999). Moreover, given the importance of the spatiotemporal aspects of NO production, the main asset of DAF-2DA/FM dyes is their capacity to detect NO at the intracellular level in real-time conditions.

However, many questions still remain that make the study of NO during the HR problematic: how and where is NO produced in this process, is it trapped in cells or does it mainly diffuse across membranes, and what are its targets? It is still not known how NO reacts in plant cells where redox balance is highly affected because of the massive concomitant oxidative burst required for triggering hypersensitive cell death. For these reasons, it seems clear that more than one method is needed to accurately quantify the NO produced in plants when challenged by a pathogen. Both intracellular and extracellular NO content should be measured in addition to detecting different forms of NO (gas, radical, or oxidative metabolites).

REFERENCES

- Archer, S. (1993). Measurement of nitric oxide in biological models. *FASEB J.* **7**, 349–360.
- Beligni, M. V., and Lamattina, L. (2001). Nitric oxide: A non-traditional regulator of plant growth. *Trends Plant Sci.* **6**, 508–509.
- Berkels, R., Purol-Schnabel, S., and Roesen, R. (2001). A new method to measure nitrate/nitrite with a NO-sensitive electrode. *J. Appl. Physiol.* **90**, 317–320.
- Bethke, P. C., Badger, M. R., and Jones, R. L. (2004). Apoplastic synthesis of nitric oxide by plant tissues. *Plant Cell* **16**, 332–341.
- Broillet, M., Randin, O., and Chatton, J. (2001). Photoactivation and calcium sensitivity of the fluorescent NO indicator 4,5-diaminofluorescein (DAF-2): Implications for cellular NO imaging. *FEBS Lett.* **491**, 227–232.
- Clarke, A., Desikan, R., Hurst, R. D., Hancock, J. T., and Neill, S. J. (2000). NO way back: Nitric oxide and programmed cell death in *Arabidopsis thaliana* suspension cultures. *Plant J.* **24**, 667–677.

- Conrath, U., Amoroso, G., Köhle, H., and Sültemeyer, D. (2004). Non-invasive online detection of nitric oxide from plants and some other organisms. *Plant J.* **38**, 1015–1022.
- Davies, M. J. (2002). Recent developments in EPR spin-trapping. *Electron Paramagn. Reson.* **18**, 47–73.
- Delledonne, M. (2005). NO news is good news for plants. *Curr. Opin. Plant Biol.* **8**, 390–396.
- Delledonne, M., Xia, Y., Dixon, R. A., and Lamb, C. (1998). Nitric oxide functions as a signal in plant disease resistance. *Nature* **394**, 585–588.
- Delledonne, M., Zeier, J., Marocco, A., and Lamb, C. (2001). Signal interactions between nitric oxide and reactive oxygen intermediates in the plant hypersensitive disease resistance response. *Proc. Natl. Acad. Sci. USA* **98**, 13454–13459.
- de Pinto, M. C., Tommasi, F., and De Gara, L. (2002). Changes in the antioxidant systems as part of the signaling pathway responsible for the programmed cell death activated by nitric oxide and reactive oxygen species in tobacco Bright-Yellow 2 cells. *Plant Physiol.* **130**, 698–708.
- Foissner, I., Wendehenne, D., Langebartels, C., and Durner, J. (2000). *In vivo* imaging of an elicitor-induced nitric oxide burst in tobacco. *Plant J.* **23**, 817–824.
- Gould, K. S., Lamotte, O., Klinguer, A., Pugin, A., and Wendehenne, D. (2003). Nitric oxide production in tobacco leaf cells: A generalized stress response? *Plant Cell Environ.* **26**, 1851–1862.
- Huang, X., Stettmaier, K., Michel, C., Hutzler, P., Mueller, M. J., and Durner, J. (2004). Nitric oxide is induced by wounding and influences jasmonic acid signalling in *Arabidopsis thaliana*. *Planta* **218**, 938–946.
- Ignarro, L. J., Fukuto, J. M., Griscavage, J. M., Rogers, N. E., and Byrns, R. E. (1993). Oxidation of nitric oxide in aqueous solution to nitrite but not nitrate: Comparison with enzymatically formed nitric oxide from L-arginine. *Proc. Natl. Acad. Sci. USA* **90**, 8103–8107.
- Itoh, Y., Ma, F. H., Hoshi, H., Oki, M., Noda, K., Ukai, Y., Kojima, H., Negano, T., and Toda, N. (2000). Determination and bioimaging method for nitric oxide in biological specimens by diaminofluorescein fluorometry. *Anal. Biochem.* **287**, 203–209.
- Jasid, S., Simontacchi, M., Bartoli, C. G., and Puntarulo, S. (2006). Chloroplasts as nitric oxide cellular source: Effect of reactive nitrogen species on chloroplastic lipids and proteins. *Plant Physiol.* **142**, 1246–1255.
- Kojima, H., Nakatsubo, N., Kikuchi, K., Kawahara, S., Kirino, Y., Nagoshi, H., Hirata, Y., and Nagano, T. (1998). Detection and imaging of nitric oxide with novel fluorescent indicators: Diaminofluoresceins. *Anal. Chem.* **70**, 2446–2453.
- Kojima, H., Urano, Y., Kikuchi, K., Higuchi, T., Hirata, Y., and Nagano, T. (1999). Fluorescent indicators for imaging nitric oxide production. *Angew. Chem. Int. Ed. Engl.* **38**, 3209–3212.
- Komarov, A. M., and Lai, C.-S. (1995). Detection of nitric oxide production in mice by spin-trapping electron paramagnetic resonance. *Biochim. Biophys. Acta* **1272**, 29–36.
- Lai, C.-S., and Komarov, A. M. (1994). Spin trapping of nitric oxide produced *in vivo* in septic-shock mice. *FEBS Lett.* **345**, 120–124.
- Lamotte, O., Gould, K., Lecourieux, D., Sequeira-Legrand, A., Lebrun-Garcia, A., Durner, J., Pugin, A., and Wendehenne, D. (2004). Analysis of nitric oxide signaling functions in tobacco cells challenged by the elicitor cryptogein. *Plant Physiol.* **135**, 516–529.
- Leshem, Y. Y., and Pinchasov, Y. (2000). Non-invasive photoacoustic spectroscopic determination of relative endogenous nitric oxide and ethylene content stoichiometry during the ripening of strawberries *Fragaria ananassa* (Duh.) and avocados *Persea Americana* (Mill.). *J. Exp. Bot.* **51**, 1471–1473.

- Maples, K. R., Sandstrom, T., Su, Y. F., and Henderson, R. F. (1991). The nitric oxide/heme protein complex as a biologic marker of exposure to nitrogen dioxide in humans, rats, and *in vitro* models. *Am. J. Respir. Cell Mol. Biol.* **4**, 538–543.
- Modolo, L. V., Augusto, O., Almeida, I. M., Magalhaes, J. R., and Salgado, I. (2005). Nitrite as the major source of nitric oxide production by *Arabidopsis thaliana* in response to *Pseudomonas syringae*. *FEBS Lett.* **579**, 3814–3820.
- Mur, L. A. J., Santosa, I. E., Laarhoven, L. J. J., Holton, N. J., Harren, F. J. M., and Smith, A. R. (2005). Laser photoacoustic detection allows in planta detection of nitric oxide in tobacco following challenge with avirulent and virulent *Pseudomonas syringae* pathovars. *Plant Physiol.* **138**, 1247–1258.
- Murphy, M. E., and Noack, E. (1994). Nitric oxide assay using hemoglobin method. *Methods Enzymol.* **233**, 240–250.
- Nagano, T. (1999). Practical methods for detection of nitric oxide. *Luminescence* **14**, 283–290.
- Nagano, T., Takizawa, H., and Hirobe, M. (1995). Reaction of nitric oxide with amines in the presence of dioxygen. *Tetrahedron Lett.* **36**, 8239–8242.
- Nagata, N., Momose, K., and Ishida, Y. (1999). Inhibitory effects of catecholamines and anti-oxidants on the fluorescence reaction of 4,5-diaminofluorescein, DAF-2, a novel indicator of nitric oxide. *J. Biochem. (Tokyo)* **125**, 658–661.
- Neill, S. J., Desikan, R., and Hancock, J. T. (2003). Nitric oxide signalling in plants. *New Phytol.* **159**, 11–35.
- Orozco-Cárdenas, M. L., and Ryan, C. A. (2002). Nitric oxide negatively modulates wound signalling in tomato plants. *Plant Physiol.* **130**, 487–493.
- Planchet, E., Jagadis Gupta, K., Sonoda, M., and Kaiser, W. M. (2005). Nitric oxide emission from tobacco leaves and cell suspensions: Rate limiting factors and evidence for the involvement of mitochondrial electron transport. *Plant J.* **41**, 732–743.
- Planchet, E., and Kaiser, W. M. (2006). Nitric oxide (NO) detection by DAF fluorescence and chemiluminescence: A comparison using abiotic and biotic NO sources. *J. Exp. Bot.* **57**, 3043–3055.
- Planchet, E., Sonoda, M., Zeier, J., and Kaiser, W. M. (2006). Nitric oxide (NO) as an intermediate in the cryptogeiin-induced hypersensitive response: A critical re-evaluation. *Plant Cell Environ.* **29**, 59–69.
- Prats, E., Mur, L. A. J., Sanderson, R., and Carver, T. L. W. (2005). Nitric oxide contributes both papilla-based resistance and the hypersensitive response in barley attacked by *Blumeria graminis f.sp. hordei*. *Mol. Plant Pathol.* **6**, 65–78.
- Qu, Z.-L., Zhong, N.-Q., Wang, H.-Y., Chen, A.-P., Jian, G. -L., and Xia, G.-X. (2006). Ectopic expression of the cotton non-symbiotic haemoglobin gene *GhHb1* triggers defense responses and increases disease tolerance in *Arabidopsis*. *Plant Cell Physiol.* **47**, 1058–1068.
- Räthel, T. R., Leikert, J. F., Vollmar, A. M., and Dirsch, V. M. (2003). Application of 4,5-diaminofluorescein to reliably measure nitric oxide released from endothelia cells *in vitro*. *Biol. Proced. Online* **5**, 136–142.
- Rockel, P., Strube, F., Rockel, A., Wildt, J., and Kaiser, W. M. (2002). Regulation of nitric oxide (NO) production by plant nitrate reductase *in vivo* and *in vitro*. *J. Exp. Bot.* **53**, 103–110.
- Tsuchiya, K., Takasugi, M., Minakuchi, K., and Fukuzawa, K. (1996). Sensitive quantitation of nitric oxide by EPR spectroscopy. *Free Radic. Biol. Med.* **21**, 733–737.
- Vandelle, E., Poinssot, B., Wendehenne, D., Bentejac, M., and Alain, P. (2006). Integrated signaling network involving calcium, nitric oxide, and active oxygen species but not mitogen-activated protein kinases in BcPG1-elicited grapevine defenses. *Mol. Plant Microbe Interact.* **19**, 429–440.

- Venkataraman, S., Martin, S. M., and Buettner, G. R. (2002). Electron paramagnetic resonance for quantitation of nitric oxide in aqueous solutions. *Methods Enzymol.* **359**, 3–18.
- Wang, J. W., and Wu, J. Y. (2004). Involvement of nitric oxide in elicitor-induced defense responses and secondary metabolism of *Taxus chinensis* cells. *Nitric Oxide* **11**, 298–306.
- Wang, J. W., and Wu, J. Y. (2005). Nitric oxide is involved in methyljasmonate-induced defense responses and secondary metabolism activities of *Taxus* cells. *Plant Cell Physiol.* **46**, 923–930.
- Wendehenne, D., Durner, J., and Klessig, D. F. (2004). Nitric oxide: A new player in plant signalling and defence responses. *Curr. Opin. Plant Biol.* **7**, 449–455.
- Yamamoto, A., Katou, S., Yoshioka, H., Doke, N., and Kawakita, K. (2004). Involvement of nitric oxide generation in hypersensitive cell death induced by elicitor in tobacco cell suspension culture. *J. Gen. Plant Pathol.* **70**, 85–92.
- Yamasaki, H., Sakihama, Y., and Takahashi, S. (1999). An alternative pathway for nitric oxide production in plants: New features of an old enzyme. *Trends Plant Sci.* **4**, 128–129.
- Zafriou, O. C., and McFarland, M. (1980). Determination of trace levels of nitric oxide in aqueous solution. *Anal. Chem.* **52**, 1662–1667.
- Zaninotto, F., La Camera, S., Polverari, A., and Delledonne, M. (2006). Cross talk between reactive nitrogen and oxygen species during the hypersensitive disease resistance response. *Plant Physiol.* **141**, 379–383.
- Zeidler, D., Zähringer, U., Gerber, I., Dubery, I., Hartung, T., Bors, W., Hutzler, P., and Durner, J. (2004). Innate immunity in *Arabidopsis thaliana*: Lipopolysaccharides activate nitric oxide synthase (NOS) and induce defense genes. *Proc. Natl. Acad. Sci. USA* **101**, 15811–15816.
- Zhang, X., Kim, W. S., Hatcher, N., Potgieter, K., Moroz, L. L., Gillette, R., and Sweedler, J. V. (2002). Interfering with nitric oxide measurements: 4,5-Diaminofluorescein reacts with dehydroascorbic acid and ascorbic acid. *J. Biol. Chem.* **277**, 48472–48478.